



LAWRENCE  
LIVERMORE  
NATIONAL  
LABORATORY

# WIDE BANDGAP EXTRINSIC PHOTOCONDUCTIVE SWITCHES

J. S. Sullivan, J. R. Stanley

August 10, 2007

Pulsed Power Conference  
Albuquerque, NM, United States  
June 18, 2007 through June 22, 2007

## **Disclaimer**

---

This document was prepared as an account of work sponsored by an agency of the United States government. Neither the United States government nor Lawrence Livermore National Security, LLC, nor any of their employees makes any warranty, expressed or implied, or assumes any legal liability or responsibility for the accuracy, completeness, or usefulness of any information, apparatus, product, or process disclosed, or represents that its use would not infringe privately owned rights. Reference herein to any specific commercial product, process, or service by trade name, trademark, manufacturer, or otherwise does not necessarily constitute or imply its endorsement, recommendation, or favoring by the United States government or Lawrence Livermore National Security, LLC. The views and opinions of authors expressed herein do not necessarily state or reflect those of the United States government or Lawrence Livermore National Security, LLC, and shall not be used for advertising or product endorsement purposes.

# WIDE BANDGAP EXTRINSIC PHOTOCONDUCTIVE SWITCHES\*

J. S. Sullivan and J. R. Stanley

*University of California  
Lawrence Livermore National Laboratory  
Livermore, CA 94550*

## *Abstract*

Semi-insulating Silicon Carbide and Gallium Nitride are attractive materials for compact, high voltage, photoconducting semiconductor switches (PCSS) due to their large bandgap, high critical electric field strength and high electron saturation velocity. Carriers must be optically generated throughout the volume of the photoswitch to realize the benefits of the high bulk electric field strength of the 6H-SiC (3 MV/cm) and GaN (3.5MV/m) materials. This is accomplished by optically exciting deep extrinsic levels in Vanadium compensated semi-insulating 6H-SiC and Iron compensated semi-insulating GaN. Photoconducting switches with opposing electrodes were fabricated on a-plane, 6H-SiC substrates and c-plane, GaN substrates. This work reports the initial fabrication and test of extrinsic GaN switches excited at a wavelength of 532 nm, and the progress made since the first phase<sup>1</sup> of switch tests of a-plane, 6H-SiC PCSS.

## **I. Introduction**

6H-SiC and 2H-GaN have wide band-gaps (3 – 3.4 eV), high critical field strength (300-400 MV/m) and high-saturated electron velocity ( $2.0 - 2.5 \times 10^7$  cm/s). These material properties make semi-insulating 6H-SiC and GaN attractive semiconductor materials for the Photoconductive Semiconductor Switch (PCSS) application. This work describes the initial investigation of 6H-SiC and GaN for use as extrinsic, photoconductive switches. Previous SiC PCSS work [2-4] used high resistivity, low impurity SiC polytypes and focused on lateral geometry surface switches that used above band-gap wavelengths of light to trigger the switches. The performance and switch life of lateral geometry PCSS are limited by surface flashover, surface carrier mobility and high current density. PCSS with opposing electrical contacts deposited on vanadium compensated, semi-insulating, 2H-GaN and 6H-SiC substrates can be triggered using below band-gap light to excite carriers from extrinsic levels throughout the bulk of the material. This results in diffuse photocurrent and switch hold off voltages determined by the bulk breakdown field strength of 2H-GaN and 6H-SiC materials. The bulk switching capability and semi-insulating nature of 6H-SiC and 2H-GaN are enabled by the addition of the dopants vanadium

and Iron. Vanadium is an amphoteric impurity that can act as a deep acceptor, or a deep donor in 6H-SiC. The local Fermi level in the 6H-SiC is determined by the relative densities of the impurities, nitrogen, boron and vanadium present in the material. Vanadium acts as a deep acceptor when the nitrogen donor impurity density sufficiently exceeds the boron acceptor impurity density, which is the case for the 6H-SiC material we have tested.

Another feature of this material is that the Fermi level will be pinned close to the Vanadium acceptor level. The deep (0.7 eV below conduction band) Vanadium acceptor levels accept electrons donated from the shallow (0.08 eV below conduction band) Nitrogen donor levels resulting in semi-insulating 6H-SiC material. The electrons residing in the extrinsic Vanadium acceptor levels can be excited into the conduction band by photons with energies exceeding 0.7 eV. Figure 1 [5] depicts the extrinsic levels in the 6H-SiC bandgap. The Boron acceptor levels and defect levels are also shown in Figure 1. The defect levels include Silicon vacancies and the UD-1 defect [5]. Semi-insulating GaN utilizes an Iron acceptor level (0.5 – 0.6 eV below the conduction band) to compensate shallow Oxygen donors. Electrons that are captured by the Iron acceptor levels can be excited into the conduction band by photons with energies greater than 0.6 eV.

## **II. Physical Limitations of Extrinsic PCSS**

An ideal high voltage switch should hold off high voltage in the off state, have negligible resistance in the on state, be easy to trigger and as small as practical. Extrinsic PCSS fabricated from 2H-GaN and 6H-SiC offer hold off voltages limited only by the critical fields of the materials (300 – 400 MV/m) and the enhancement factor of the switch electrode geometry. Devices based on 1 mm thick substrates can hold off tens of kilovolts. The on resistance of 6H-SiC and 2H-GaN extrinsic PCSS is limited by the number of carriers that are trapped in extrinsic levels of the material and the active area of the device. The carriers trapped in the extrinsic levels are limited to the  $10^{16} - 10^{17}/\text{cm}^3$  range, but this is sufficient to achieve sub-ohm on resistance for a switch area of a few  $\text{cm}^2$ . Applying an optical pulse to one, or more, of its facets, triggers the switch. Currently, 6 – 10 mJ of optical energy is required to trigger the device, but this will be reduced by the optimization of impurity levels. The physical size of the switch is limited by the required

hold off voltage and the penetration depth of the optical trigger pulse.

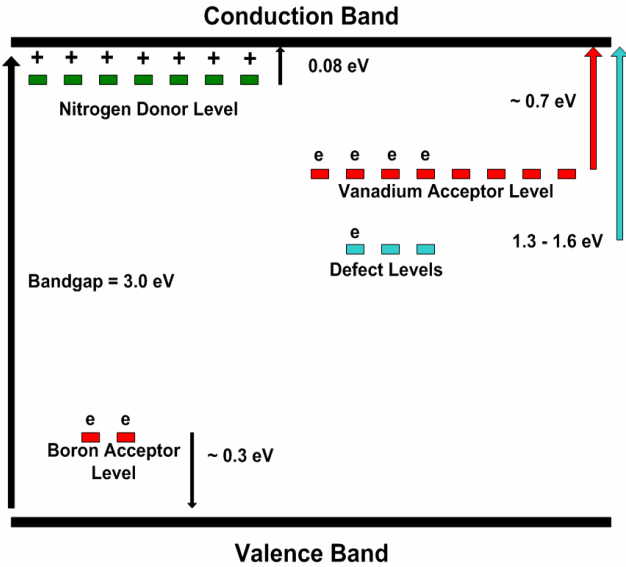


**Figure 1.** Vanadium acceptor and nitrogen donor levels in vanadium compensated 6H-SiC.

### III. 6H-SiC Switch Test Results

A detailed presentation of the 6H-SiC switch test results has been previously reported [1]. Here we will present a brief review. Six PCSS devices were fabricated from samples of 400  $\mu\text{m}$  thick, 1.2 cm per side, square substrates of “a” plane, vanadium compensated, semi-insulating 6H-SiC. The four facets of the substrate were cleaved/polished to enhance optical coupling into the bulk of the substrate. The contacts consist of a 0.8 cm diameter, circular metalization centered on opposing sides of the substrate. The metalization formed an ohmic contact and consisted of layers of nickel, titanium, platinum and gold. The metal deposition and anneal were performed at SemiSouth Laboratories Inc. in Starksville, MS. Indium coated copper electrodes were brazed to the substrate metalizations to facilitate electrical connection. The finished 6H-SiC PCSS assembly is shown in Figure 2. Photoconductivity tests were performed using 1064 nm and frequency doubled 532 nm wavelength light from a Q-switched Nd:YAG laser with an 8 ns at full wave half maximum (FWHM) output pulse. The optical pulse was focused and aligned to obtain as uniform as possible light pulse over a rectangular area measuring 1 cm wide by 400  $\mu\text{m}$  high. The optical pulse was then centered on the PCSS facet. Photoconductivity tests were performed using optical pulse energies ranging from 1 to 14 mJ.

The photoconductivity of the PCSS was measured using the circuit shown in Figure The 1.5  $\mu\text{F}$  capacitor of the test circuit was pulse charged to bias voltages ranging from 250 V to 4.25 kV in 30  $\mu\text{s}$  and the PCSS was optically triggered after a 30  $\mu\text{s}$  flat top interval of the

pulse bias voltage for the 6H-SiC device. The voltage across the PCSS was measured differentially using a pair of calibrated, fast (250 MHz bandwidth), high voltage (5 kV) probes. The load voltage was measured using a fast (35 ps rise time), low impedance (250  $\Omega$ ) high voltage probe. The PCSS current was obtained by dividing the load voltage by the load resistance. Dynamic switch resistance is another important switching parameter. The dynamic switch resistance is calculated by dividing the switch voltage by the load current.



**Figure 2.** Vanadium compensated, semi-insulating, 6H-SiC PCSS assembly.

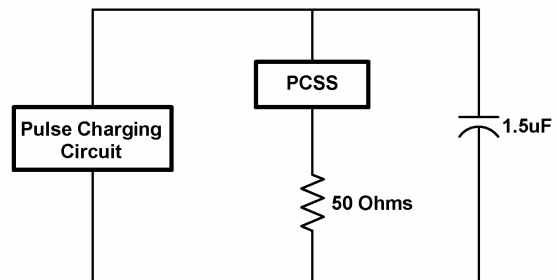


**Figure 3.** Simple schematic for PCSS photoconductivity test circuit.

The PCSS voltage and current for a 4.25 kV charge voltage and optical pulse energy of 13 mJ at 1064 nm are shown in Figure 4. The PCSS voltage starts at 4.25 kV and collapses to approximately 750 Volts in 10 ns, while the PCSS current increases from zero to 70 A. The PCSS current pulse is increases from zero to 70 A. The PCSS current pulse is similar in temporal profile to the 1064 nm optical trigger pulse. However, the photocurrent has a 16 ns FWHM pulse- width indicating a carrier recombination time of a few nanoseconds, or, less. The minimum dynamic PCSS resistance for the pulse shown in Figure 4 is 11  $\Omega$ . The minimum dynamic PCSS resistance is approximately constant for fixed optical pulse energy, regardless of the charge voltage. Switch minimum dynamic PCSS resistance as a function of optical pulse energy for 1064 and 532 nm wavelengths is shown in

Figure 5. The switch minimum dynamic PCSS resistance decreases rapidly with optical pulse energy for both

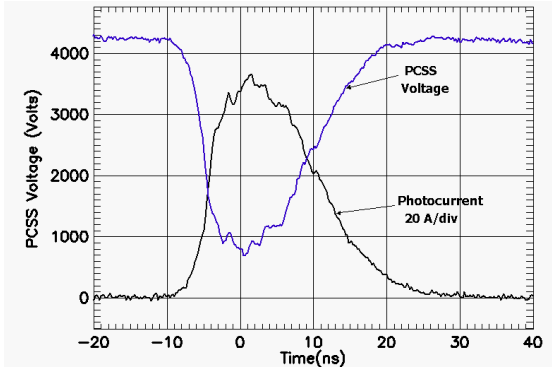


Figure 4. PCSS voltage and current for bias voltage of 4.25 kV and 13 mJ optical trigger at 1064 nm.

optical wavelengths. The PCSS attains a lower minimum dynamic resistance at all optical energies for excitation with 532 nm light compared to excitation with 1064 nm light. This is a result of charge carriers being excited from additional extrinsic levels by the 532 nm wavelength.

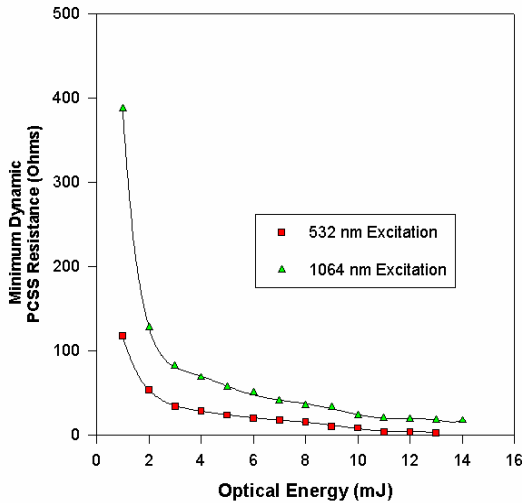


Figure 5. Minimum dynamic PCSS resistance as function of optical trigger energy for 532 and 1064 nm.

There are carriers excited at the 532 nm wavelength that have a significantly different lifetime than that of the remaining carriers. This is captured in Figure 6. The most notable difference is the long tail on the photocurrent excited at 532 nm. The current tail persists and for one PCSS took approximately one millisecond to decay to zero. We believe crystal defects, that act as electron traps [5, 7] located 1.3-1.6 eV below the conduction band, are contributing the carriers in the photocurrent tail. Electrons are captured by the traps and thermally excited back into the conduction band resulting in a long decay time. The electron trap level has a recovery time of from a few up to 200  $\mu$ s.

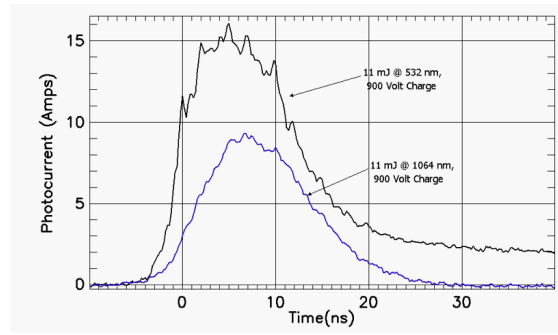


Figure 6. PCSS photocurrent temporal pulse for 11 mJ optical excitation at 532 and 1064 nm wavelengths.

#### IV. SiC and GaN Transmission Measurements

Optical transmission measurements were performed on a 7.2 mm by 3.7 mm, 400  $\mu$ m thick, 6H-SiC substrate and a 9.0 mm by 9.0 mm, 408  $\mu$ m thick, 2H-GaN substrate. The optical pulse passed through a 50/50 beam splitter and half the pulse was applied to a SiC, or GaN, substrate facet and the other half was applied to an optical energy meter. Optical pulses were applied to the 3.7 mm by 400  $\mu$ m facet of the 6H-SiC substrate with the optical E field vector perpendicular to the c direction of the SiC crystal. For the GaN substrate, the optical pulse was applied to the 9.0 mm by 408  $\mu$ m facet with the optical E field vector parallel to the c direction of the GaN crystal. Both substrates were masked so that only light striking the facet was transmitted to an optical energy meter positioned behind it. The effective absorption was calculated from the transmission measurements using measured values of the index of refraction [8,9] and assuming linear absorption and using equation (1)

$$T = \frac{\left(1 - \left(\frac{n-1}{n+1}\right)^2\right)^2 \exp(-\alpha l)}{1 - \left(\exp(-\alpha l) \left(\frac{n-1}{n+1}\right)^2\right)^2} \quad (1)$$

Where T is the transmission,  $\alpha$  is the effective linear absorption, l is the length traveled through the substrate and n is the index of refraction of either 6H-SiC or GaN. Plots of the effective absorption as a function of optical energy are shown in Figures 7 and 8. It is apparent from the plots that the absorption has a nonlinear component. We assume that the largest nonlinear component of the absorption is free carrier absorption. The materials with the largest nonlinear component indicate the better switch material at the given wavelength. On the other hand higher absorption translates to shallower optical penetration depths and smaller switch structures.

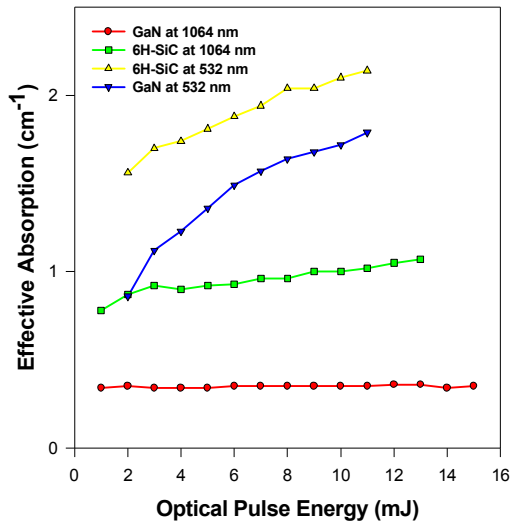


**Figure 7.** Effective optical absorption in GaN and SiC at 532 and 1064 nm

### V. GaN Switch Testing

A GaN switch assembly was fabricated using a 9 mm by 9 mm, 408  $\mu\text{m}$  thick, semi-insulating substrate. The GaN substrate was epitaxially grown by Kyma Technologies. 6.5mm diameter circular metallization layers were centered on both sides of the GaN substrate. The metallization consisted of layers of Titanium and Gold deposited by a liftoff technique. Copper electrodes were brazed to the substrate metallization using Indium solder. The GaN switch assembly is shown in Figure 8.

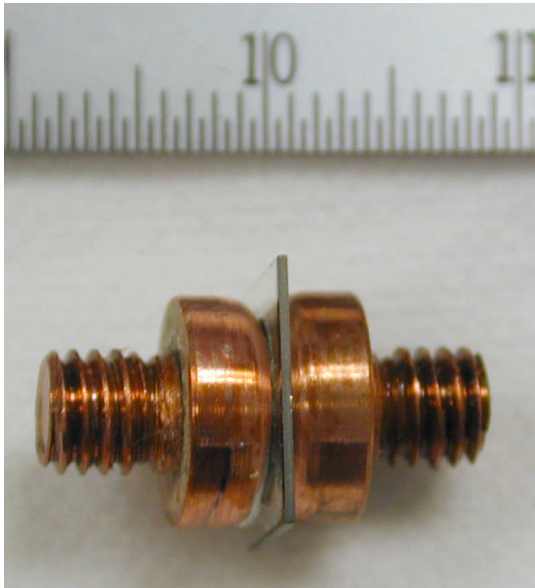


**Figure 8.** GaN switch assembly (ruler scale in mm)

The GaN device was tested using the same circuit as the 6H-SiC devices (Fig.3) with a range of bias voltages from

150 to 1000 volts. Optical excitation at both 532 and 1064nm were applied to the GaN switch. However, only a negligible amount of photocurrent was generated at 1064 nm. The results for excitation at 532 nm are shown below. Figure 9 shows the GaN switch voltage, current and optical excitation for a 1000 Volt charge voltage and 12 mJ of optical excitation at 532 nm. These results were obtained for an optical pulse that measured  $\sim 5.5\text{ns}$  (FWHM) significantly shorter than the optical pulses used to excite the 6H-SiC switch (8 ns FWHM).

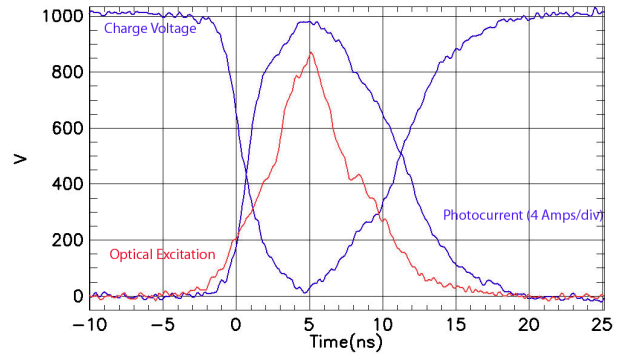


**Figure 9.** Switch voltage, photocurrent and optical excitation for GaN switch at 1000 Volts charge voltage and 12 mJ excitation at 532 nm.

The general results of the GaN switch testing are summarized in Figures 10 and 11. Figure 10 shows the peak switch photocurrent as a function of optical excitation energy at a wavelength of for a variety of charge voltages. The saturation of the photocurrent begins at 3 – 4 mJ of optical excitation for all charge voltages.

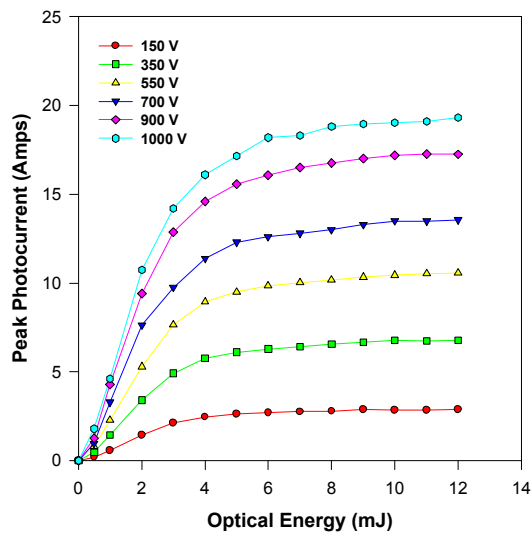


**Figure 10.** Peak photocurrent of GaN switch as function of optical excitation energy for range of charge voltages of 150 – 1000 Volts.

The data shown in Figure 10 can be recast to show the peak photocurrent as a function of charge voltage for a

range of optical excitation energies. The resulting plots are shown in Figure 11 and the linear nature of the GaN switch becomes apparent. The peak photocurrent is a linear function of bias voltage for excitation with a fixed optical energy. This indicates that the total resistance of the test circuit is constant for a fixed applied optical energy. The circuit resistance calculated for a fixed applied optical energy of 0.5 and 12 mJ is 685.7 and 51.6 Ohms, respectively. The minimum GaN switch resistance is calculated by subtracting the 51 Ohm load resistance from the total circuit resistance, resulting in 634.7 and 0.6 Ohms, respectively for 0.5 and 12 mJ excitation.

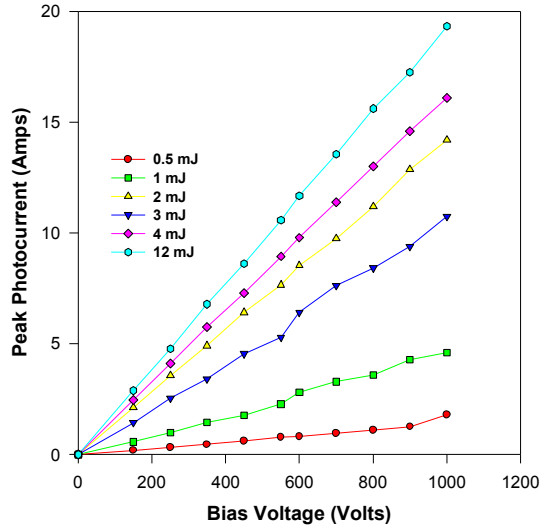


**Figure 11.** Peak photocurrent vs bias voltage for a range of 0.5 – 12 mJ in optical energies.

## VI. Conclusions

Linear, extrinsic photoconductive switches have been fabricated from semi-insulating 6H-SiC and 2H-GaN substrates. Minimum switch resistances of 11 and 2 –3 Ohms have been demonstrated for 6H-SiC devices at 1064 and 532 nm excitation, respectively. Minimum switch resistances of 1100 and 0.6 Ohms have been demonstrated for a 2H-GaN device at 1064 and 532 nm excitation, respectively. It appears that the shallow Nitrogen donor and deep Vanadium acceptor levels are key to the switching at 1064 nm in the 6H-SiC devices. Unknown deeper levels contribute to the long tail in the photocurrent in the SiC devices at 532 nm. The expected switching action using the shallow Oxygen donor and deep Iron acceptor levels in 2H-GaN was never manifested at 1064 nm excitation. Unknown deep levels exhibited strong switching action in GaN at 532 nm excitation. Future work will be to optimize the Nitrogen and Vanadium density in 6H-SiC for switching at 1064 nm, identify levels that contribute to the tail in the photocurrent in SiC at 532 nm and identifying deep levels in GaN that contribute to switching at 532 nm.

## VII. References

- [1] J. Sullivan and J. Stanley, "6H-SiC Photoconductive Switches Triggered at Below Bandgap Wavelengths", IEEE Transactions on Dielectrics and Electrical Insulation, volume 14, issue 4, August, 2007.
- [2] S. Dogan, A. Teke, D. Huang, H. Morkoc, C. Roberts, J. Parish, B. Ganguly, M. Smith, R. Myers and S. Sadow, "4H-SiC photoconductive switching devices for use in high-power applications", Appl. Phys. Letts., Vol. 82, pp. 3107-3109, 2003.
- [3] S. Sheng, M. Spencer, X. Tang, P. Zhou and G. Harris, "Polycrystalline cubic silicon carbide photoconductive switch", IEEE Electron Device Letts., Vol. 18, pp 372-374, 1997.
- [4] K. Zhu, S. Dogan, Y. Moon, J. Leach, F. Yun, D. Johnstone, H. Morkoc, G. Li and B. Ganguly "Effect of n<sup>+</sup>-GaN subcontact layer on 4H-SiC high-power photoconductive switch", Appl. Phys. Letts. 86, p. 261108, 2005.
- [5] M. Bickermann, D. Hofmann, T. Straubinger, R. Weingartner and A. Winnacker, "Preparation of semi-insulating Silicon Carbide by Vanadium doping during PVT bulk crystal growth", Materials Science Forum, Vol. 433-436, pp. 51-54, 2003.
- [6] P. Cho, J. Goldhar, C. Lee, S. Sadow and P. Neudeck, "Photoconductive and photovoltaic response of high-dark-resistivity 6H-SiC devices", J. Appl. Phys., Vol. 77, pp. 1591-1599, 1995.
- [7] T. Dalibor, G. Pensl, H. Matsunami, T. Kimoto, W. Choyke, A. Schoner and N. Nordell, "Deep defect centers in Silicon Carbide monitored with deep level transient spectroscopy", Physica Status Solidi (A) Appl. Research, Vol.162, pp. 199-225, 1997.
- [8] E. Palik, *Handbook of Optical Constants of Solids*, p 593, Academic Press, 1985
- [9] M. Lin, B. Sverdlov, S. Strite, H. Morkoc and A. Drakin, "Refractive indices of wurtzite and zinblende GaN", Electronics Letters, vol. 29, no. 20, September 1993

**James S. Sullivan** received the B.E.E. degree from Manhattan College, Riverdale, NY and the M.S.E.E. degree from the State University of New York at Buffalo in 1977 and 1980, respectively. Since 1983 he has been an electrical engineer at the Lawrence Livermore National Laboratory, Livermore, CA. His research interests include optoelectronics, semiconductors and high voltage switching.

**Joel R. Stanley** received his AAS in Laser Electro-Optics from Texas State Technical College (TSTC), Waco, TX in 1995. He has been employed with Lawrence Livermore National Laboratory, Livermore, CA since 2001. His research interests include: laser optics and high voltage transmission line pulsers.